Switched-Capacitor Based Implantable Low-Power Wireless Microstimulating Systems

Maysam Ghovanloo[1,2]

[1]Department of Electrical and Computer Engineering, [2]Department of Biomedical Engineering,
North Carolina State University, Raleigh, NC, USA
mghovan@ncsu.edu

Abstract— **The main objective of this paper is to introduce a new category of implantable wireless microstimulators based on discharging a series of small capacitors to inject quantized lumps of electric charge into the excitable tissue, namely *Switched-Capacitor based micro-Stimulators* (SCS). In this method, the total amount of charge per stimulation phase can be controlled by changing the initial and final capacitor voltages as well as the number of capacitors being discharged. The rate of discharge, which is the stimulus current, is also a controllable parameter that adds more flexibility to this stimulation approach, while improving the implant safety. The key reason for adopting SCS in implantable low-power devices was to combine the power efficiency of the voltage-controlled stimulators (VCS) with the safety and stimulation parameter controllability of the current-controlled stimulation (CCS) circuits. In addition, the SCS technique substantially simplifies the microstimulator architecture, and depending on the application, can potentially reduce the implant size and power requirements. It also provides an opportunity to apply different stimulus waveforms to the excitable tissue that can be more efficacious in activating the surrounding nerve or muscle fibers compared to the commonly used square-shaped pulses.**

I. Introduction

There are many existing and emerging therapies using implantable wireless electrical stimulators to alleviate cardiac dysfunctions, sensory deficits, paralysis, and tremor [1]-[4]. Shrinking the size of implantable stimulating devices such as pacemakers, cochlear implants, visual prosthesis, and deep brains stimulators (DBS) to reduce the invasiveness of these devices, alleviate post surgical complications, improve their safety, and increase the popularity of these devices among patients [1] is a major goal in the field of implantable microelectronics.

About half of the volume inside the metallic can of an existing battery-powered implant is filled with electronic components and the other half is occupied by a non-rechargeable extended lifetime battery that should last for more than 5 years. The best way to shrink the size of electronics is to approach full-integration by incorporating all of the required circuitry on a single chip (system-on-a-chip or SoC), thus minimizing the number of discrete off-chip components. This was the approach we adopted in development of the Interestim-2B, which is an implantable modular wireless microstimulating system with large number of sites for visual and auditory neuroprostheses [3], [4]. Shrinking the size of the battery, however, is more challenging due to its limited energy storage density. Two solutions can be considered to reduce the battery size:

First, keeping the main energy source out of the body. This can be done by replacing the permanent non-rechargeable battery, which has to store enough energy for several years; with a smaller rechargeable battery that stores only enough energy for several days or weeks. To recharge the implanted battery, the external primary energy source generates an alternating magnetic field that is inductively coupled to an internal power supply through a pair of coils that constitute a transformer. Therefore, the internal battery will be recharged when the patient wears the external power transmitter for several hours in a convenient time.

Second, reducing the stimulator power consumption. This can result in a smaller size, less frequently charged, and longer lifetime battery. There are two sorts of power consumption in an implantable microstimulator: A smaller part of the power drained from the battery is consumed in the microstimulator internal circuitry, resulting in heat dissipation. A larger portion of the power is transferred into the tissue through stimulus pulses. The internal power consumption can be reduced by lowering the operating voltages and utilizing low-power circuit design techniques [5]. The amount of transferred power into the tissue that is needed to induce the desired neurological effect depends on many factors including the stimulation front-end (SFE) circuitry, stimulus waveforms, stimulation frequency, excitation thresholds of the targeted excitable tissue, and stimulating electrodes location, configuration, geometry, surface property, and coating material (electrode-electrolyte interface) [6]. The focus of this article is on the architecture of the SCS implant and its stimulus waveforms. The ultimate goal is to improve the efficacy of the stimulation pulses by minimizing the amount of battery power needed to elicit the desired physiological response, including initiation or suppression of action potentials.

II. Stimulation Strategies

The stimulator instantaneous output power (into the tissue) can be calculated by multiplying the voltage, V, across two active electrodes (in bipolar stimulation) or one active electrode and a distant ground electrode (in monopolar stimulation) by the current, I, that flows between

them. V and I are simply related by the sum of tissue and electrodes impedances, Z, according to the Ohm's law. However, the main source of complexity is in the Z value, which is resistive-capacitive, highly nonlinear, and in many cases variable with time, frequency, and tissue reactions [6].

In conventional multichannel microstimulators, the SFE circuitry selects the active electrodes and controls either the voltage or the current between them. In voltage-controlled stimulation (VCS), the SFE circuit applies a certain voltage, V, across the two electrodes. The current, I, passing through the tissue in this case only depends on Z. Therefore, this method is only used when the range of Z variations over time or from one pair of electrodes to another is small and well known. The stimulator voltage, V, can be programmed within safe limits by the physician in order to achieve the desired neurophysiologic response. The SFE circuitry in this case has little control over the stimulus current, except for limiting it to safe levels in order to eliminate irreversible Faradic chemical reactions. The efficiency of the VCS is higher when the stimulation voltage is close to the battery voltage. However, it degrades when higher or lower voltages are needed. Several variations of the VCS-SFE have been discussed in [7]-[9].

In current-controlled stimulation (CCS), the stimulus current, I, is programmed by the physician. The SFE circuitry automatically controls the voltage, V, across the two active electrodes such that the desired current, I, passes through the tissue. This method is more suitable when Z varies in a wide range, especially in microstimulation with miniature electrodes [3], because the CCS circuitry keeps I constant regardless of Z variations. The only exception is when the voltage required to pass I through a large Z is above the maximum available SFE output voltage, known as the SFE voltage compliance. In this case, the SFE current source saturates and I does not reach the desired level.

In general, VCS circuits are simpler and more power efficient than CCS. The latter, however, is safer and provides better control over the amount of charge injected into the tissue as a result of $Q_{CS} = I \times T_P$, where Q_{CS} is the injected charge and T_P is the stimulus pulse duration. Some recent studies also suggest that CCS might be more effective than VCS in the neural tissue excitation [10]. Pacemakers are VCS-based and most existing DBS implants, which technologies are mainly inherited from pacemakers, also use VCS method. However, VCS should be used with caution due to the absence of charge control. As a result, manufacturers must indicate the safety limits by providing curves and data tables in terms of the electrode-tissue impedance. An example is shown in Fig. 1 [11].

We are developing a wireless implantable switched-capacitor based stimulation (SCS) system by combining the power efficiency and simplicity of a VCS with the safety and charge injection controllability of a CCS (see Fig. 3). The SCS system involves charging a group of capacitors

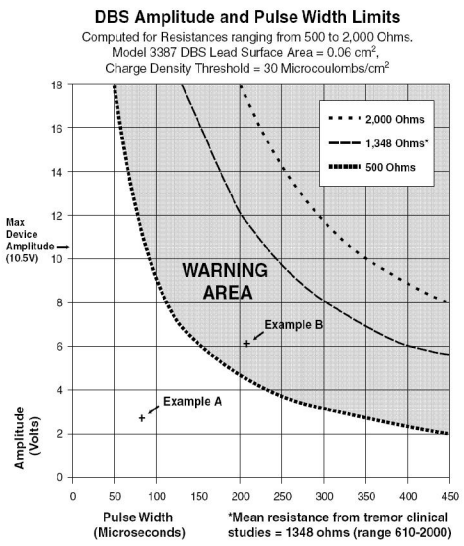

Fig. 1. Published manufacturer safety limits of a VCS-based DBS implant as indicated by electrode/tissue impedance curves [11].

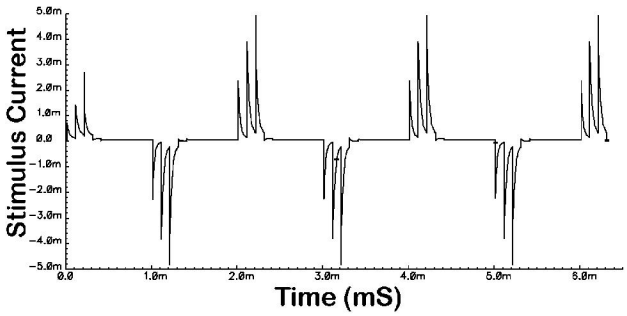

Fig. 2. Switched-capacitor based microstimulator simulated bipolar-biphasic stimulus current waveform through a resistive load.

from a rechargeable battery by means of a DC to DC converter, and discharging them into the excitable tissue through multiple electrodes by means of a plurality of switches that are digitally controlled. The maximum capacitor discharge current is also controllable by a current source. The total amount of injected charge over each stimulation phase period is measured by integrating the stimulus current, and used for charge balancing, which is a necessary safety feature in implantable microstimulators [6].

Using the SCS implant we can control the stimulus timing, voltage, current, and amount of charge being injected into the tissue. Fig. 2 shows the unique exponential waveforms generated by the SCS implant. In some applications, such as DBS, these waveforms may prove to be more efficacious than the common square-shaped stimulus pulses due to comprising of both high and low frequency components at the output spectrum as well as providing large voltage compliance [12]-[14].

III. SCS Implant Architecture

Fig. 3a shows the SCS implant block diagram. It can be seen that major blocks, enclosed in grey boxes, will be

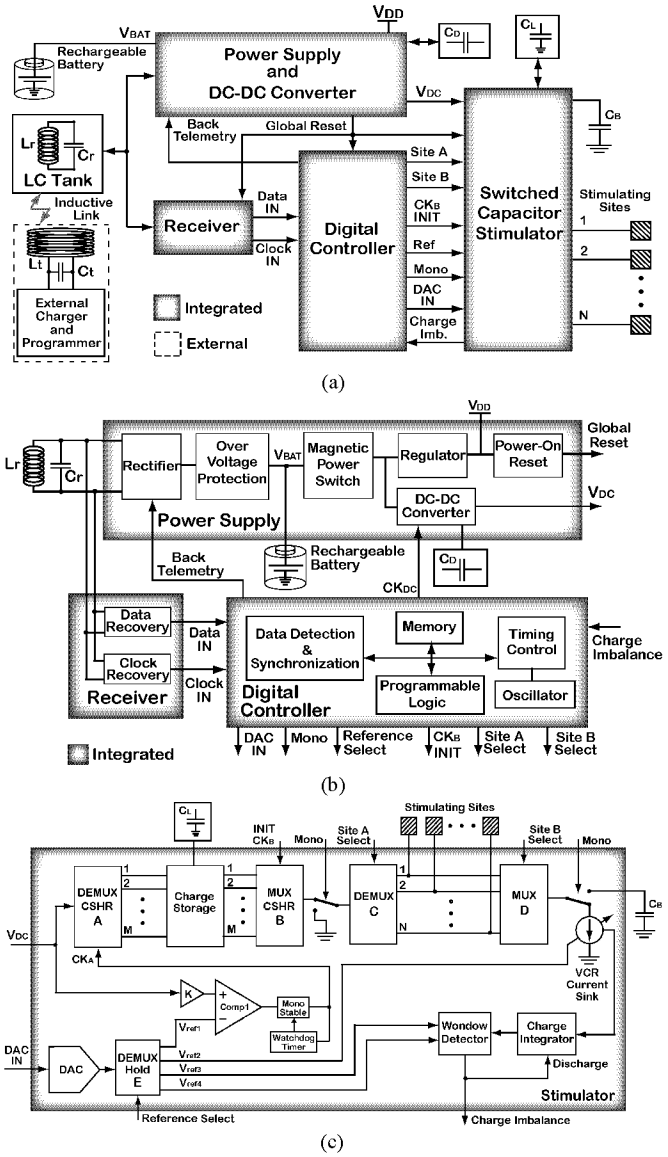

Fig. 3. (a) Overall block diagram of the implantable low-power wireless switched-capacitor based microstimulating system, indicating the integrated and off-chip components of the device as well as the inductive link and the external charger/programmer unit. (b) Power supply, receiver, and digital control block diagrams. (c) Switched-capacitor based stimulation front-end (SFE) block diagram.

integrated on a single chip similar to Interestim-2B [4]. The off-chip components include a small rechargeable battery, a receiver inductive-capacitive (L_rC_r) tank circuit for charging the battery, programming, and back-telemetry, 3 capacitors associated with the power supply, and between 3 to 17 capacitors for the SFE depending on the application and maximum rate of stimulation. Even though there are up to 21 capacitors used in the SCS implant, the availability of high-CV, low-leakage current tantalum chip capacitors with capacities of up to 10 µF in 0402 package ($1\times0.5\times0.5$ mm^3), keeps the implant size very small [15], [16]. In fact the total volume of these 21 capacitors and their spacing is less than half of the estimated chip volume ($4.6\times4.6\times0.5$ mm^3).

Fig. 3b shows the power supply, receiver, and digital controller blocks in more detail. Most of these blocks are discussed in [3], [4]. The magnetic power switch includes an integrated Hall-effect sensor and a latch, which turn the implant on and off in the presence of a DC magnetic field [17]. The DC-DC converter charges the SFE capacitors (C_L) up to an externally programmable level, V_{DC}. It also compensates V_{BAT} variations over time, which eliminates the need for a series regulator and results in power saving. The DC-DC converter can be implemented in the form of a charge pump, a voltage multiplier, or a switching regulator with high efficiency. The efficiency of the DC-DC converter in charging its fully capacitive loads has a significant effect on the overall efficiency of the SCS system [18].

Fig. 3c shows the switched-capacitor based SFE circuitry, which consists in part of a group of equal charge storage capacitors C_{L1}-C_{Lm}. One terminal of each charge storage capacitor is grounded. The other terminal of each C_{L1}-C_{Lm} capacitor, C_{Li}, is controlled by a switch with the following states:

1- Connected to the DC-DC output through DEMUX-A, while C_{Li} is being charged up to V_{DC}.

2- At high-impedance to preserve charge till the onset of stimulation is defined by the internal control circuitry.

3- Connected to one of the stimulator active electrodes (Sites-A) through MUX-B and DEMUX-C to discharge and inject an exponentially decaying stimulus into the excitable tissue. In biphasic stimulation, a return path for the injected charge is formed by simultaneously connecting the other active electrode (Site-B) to the stimulator ground, through MUX-D and a voltage controlled resistor (VCR) current sink [19].

The SCS-SFE in Fig. 3c also allows monophasic stimulation under control of the Mono signals, which are generated by the digital controller block. When monophasic stimulation is active, MUX-D output is connected to a blocking capacitor, C_B, instead of the VCR current sink. As a result, during stimulation the stimulus current passes through the active sites and charges C_B. Then during the interval between two successive pulses, Mono signals connect DEMUX-C input to ground and C_B gradually discharges through the same active sites to satisfy charge balancing requirement.

VCR Current Source and Charge Integrator

The VCR current source used in SCS as part of the SFE circuitry requires only a small headroom voltage (<150 mV), which maximizes the amount of useful output voltage across the active electrodes [19]. The VCR serves two purposes: First, it limits the exponential capacitive discharge stimulus current to a certain level, I_{Sink}, which is externally programmable. The current limit provides more control over the stimulus current waveform and also improves implant

safety by limiting the stimulating site charge injection density, especially at the onset of the capacitive discharge when the stimulus current is at its peak [20], [21].

For the exponential stimulus current values that are smaller than I_{Sink}, the VCR current source is almost transparent and acts only as a small series resistor for the second purpose, which is charge measurement. The VCR converts the instantaneous stimulus current that passes through the tissue to a voltage. This voltage can then be converted to a small current and integrated over the stimulation period to measure the injected charge per stimulus phase. The integrator output is compared against two programmable reference voltages, V_{ref3} and V_{ref4} in a window detector, which indicate the maximum positive and negative tolerable charge imbalance. If the integrator output exceeds these limits, the charge imbalance flag will be activated and the digital control block will try to balance the injected charge, based on preprogrammed routines, in the subsequent stimulus pulses.

V. Conclusions

We have undertaken a new approach in development of an implantable wireless microstimulating system that is based on discharging a series of small capacitors to inject quantized lumps of electric charge into the excitable tissue. The new switched-capacitor based microstimulator (SCS) combines the power efficiency and simplicity of voltage controlled stimulators (VCS) with the safety and charge injection controllability of current controlled stimulators (CCS). The SCS implant architecture is simple and depending on the application, can potentially reduce the implant size and power requirements.

SCS provides an opportunity to apply to the excitable tissue different stimulus waveforms that are based on charge injection. In a certain number of applications that need high frequency components such as DBS, these waveforms might prove to be more efficacious in activating the surrounding neural tissue compared to the commonly used square-shaped pulses. We are currently developing a prototype system that would allow us to evaluate and compare the efficacy and efficiency of three stimulation techniques using VCS, CCS, and SCS circuits. Our methodology will be to apply various stimulation waveforms using each of the three circuits and evaluate the results in terms of neurophysiologic response and required battery power. We have already started short-term *in vitro* experimental measurements on brain slices prepared from mouse somatosensory cortex using Interestim-2B [3], [4]. The preliminary results of these experiments were presented in [22].

References

[1] J. Cavuoto, "Neural engineering's image problem," *IEEE Spectrum*, vol. 41, pp. 32-37, Apr. 2004.

[2] A.L. Benabid ., B. Wallace, J. Mitrofanis, C. Xia, B. Piallat, V. Fraix, A. Batir, P. Krack, P. Pollak, and F. Berger, "Therapeutic electrical stimulation of the central nervous system," C.R. Biologies, in press, Available online: www.sciencedirect.com.

[3] M. Ghovanloo, "A wireless microsystem for neural stimulating microprobes," Ph.D. dissertation, Department of Electrical Engineering and Computer Science, University of Michigan, Ann Arbor, Jul. 2004.

[4] M. Ghovanloo and K. Najafi, "A modular 32-site wireless neural stimulation microsystem," *IEEE J. Solid-State Circuits*, vol. 39, no. 12, pp. 2457-2466, Dec. 2004.

[5] J.D. Meindl, "Low power microelectronics: retrospect and prospect," *Proc. of the IEEE*, vol. 83, pp. 619-635, Apr. 1995.

[6] D.R. Merrill, M. Bikson, and J.G.R. Jefferys, "Electrical stimulation of excitable tissue: design of efficacious and safe protocols," *J. Neuroscience Methods*, vol. 141, pp. 171-198, Feb. 2005.

[7] L.S.Y. Wong, S. Hossain, A Ta, J. Edvinsson, D.H. Rivas, H. Naas, "A very low-power CMOS mixed-signal IC for implantable pacemaker applications," *IEEE J. Solid-State Circuits*, vol. 39, no. 12, pp. 2446-2456, Dec. 2004.

[8] S.K. Kelly, J. Wyatt, "A power-efficient voltage-based neural tissue stimulator with energy recovery," *IEEE Digest Intl. Solid-State Cir. Conf.*, pp. 228-524, Feb. 2004

[9] M. Schwarz, M. Maschmann, "Area saving stimulator cells for multielectrode arrays featuring adaptive waveform generation and monitoring," *Proc. IEEE Eng. in Med. Biol. Conf.*, vol. 2, pp. 4314-4317, 2004.

[10] W.M. Grill presentation, Neural Interfaces Workshop, National Institute of Neural Disorders and Stroke, NIH, DC, Nov. 2004.

[11] Medtronic Inc., "Soletra 7460, MemoryMod software cartridge for deep brain stimulation," *application manual*, 2003

[12] J. Gimsa, B. Habel, U. Schreiber et al., "Choosing electrodes for deep brain stimulation experiments - electrochemical considerations," *J. Neuroscience Methods*, vol. 142, pp. 251-265, Mar. 2005.

[13] A.M. Kuncel, W.M. Grill, "Selection of stimulus parameters for deep brain stimulation," Clinical Neurophysiology, vol. 115, pp. 2431-2441, Jul. 2004.

[14] W.M. Grill and J.T. Mortimer, "The effect of stimulus pulse width duration on selectivity of neural stimulation," *IEEE Trans. Biomed. Eng.*, vol. 43, no. 2, pp. 161-166, Feb. 1996.

[15] Editorial electronics report, "Tantalum capacitor", *Appliance Magazine*, Feb. 2005, Available: http://www.appliancemagazine.com

[16] AVX tantalum and niobium oxide capacitors, version 2.1, AVX corporation, Oct. 2005, Available: http:/www.avx.com

[17] H.P. Baltes, R.S. Popovic, "Integrated semiconductor magnetic field sensors," *Proc. IEEE*, vol. 74, pp. 1107-1132, Aug. 1986.

[18] S. Paul, A.M. Schlaffer, J.A. Nossek, "Optimal charging of capacitors," *IEEE Trans. Cir. Sys.*, vol. 47, pp. 1009-1016, Jul. 2000.

[19] M. Ghovanloo and K. Najafi, "A compact large voltage compliance high output impedance programmable current source for biomedical implantable microstimulators," *IEEE Trans. Biomed. Eng.*, vol. 52, pp. 97-105, Jan. 2005.

[20] L.S. Robblee and T.L. Rose, "Electrochemical guidelines for selection of protocols and electrode materials for neural stimulation," in *Neural Prostheses: Fundamental Studies*, W.F. Agnew and D.B. McCreery, Eds. Englewood Cliffs, NJ: Prentice-Hall, 1990, ch. 2, pp. 26–66.

[21] J.D. Weiland and D.J. Anderson, "Chronic neural stimulation with thin-film, iridium oxide electrodes," *IEEE Trans. Biomed. Eng.*, vol. 47, no. 7, pp. 911-918, July 2000.

[22] M. Ghovanloo, O. Favorov, R.W. Murrow, and M. Tommerdahl, "Development of a switched-capacitor based neurostimulating system for low-power head-mounted deep brain stimulators," Presented at the NIH-NINDS Neural Interfaces Workshop in DC, Sep. 2005.